Int. J. Radiation Oncology Biol. Phys., Vol. 51, No. 4, pp. 1159–1166, 2001

0360-3016/01/$–see front matter

ELSEVIER

PII S0360-3016(01)01768-0

PHYSICS CONTRIBUTION

DOSIMETRIC VERIFICATION OF A DEDICATED 3D TREATMENT PLANNING SYSTEM FOR EPISCLERAL PLAQUE THERAPY

STIG KNUTSEN, M.SC.,* RUNE HAFSLUND, M.SC.,* ODD R. MONGE, M.D.,† HARALD VALEN, M.SC.,* LUDVIG PAUL MUREN, M.SC.,*‡ BERNT LOUNI REKSTAD, M.SC.,* JØRGEN KROHN, M.D.,§ AND OLAV DAHL, M.D., PH.D.‡

Departments of *Radiophysics, †Oncology, and §Ophthalmology, and ‡Section of Oncology, Institute of Medicine, Haukeland University Hospital, Bergen, Norway

Purpose: Episcleral plaque therapy (EPT) is applied in the management of some malignant ocular tumors. A customized configuration of typically 4 to 20 radioactive seeds is fixed in a gold plaque, and the plaque is sutured to the scleral surface corresponding to the basis of the intraocular tumor, allowing for a localized radiation dose delivery to the tumor. Minimum target doses as high as 100 Gy are directed at malignant tumor sites close to critical normal tissues (e.g., optic disc and macula). Precise dosimetry is therefore fundamental for judging both the risk for normal tissue toxicity and tumor dose prescription. This paper describes the dosimetric verification of a commercially available dedicated treatment planning system (TPS) for EPT when realistic multiple-seed configurations are applied.

Materials and Methods: The TPS Bebig Plaque Simulator is used to plan EPT at our institution. Relative dose distributions in a water phantom, including central axis depth dose and off-axis dose profiles for three different plaques, the University of Southern California (USC) #9 and the Collaborative Ocular Melanoma Study (COMS) 12-mm and 20-mm plaques, were measured with a diode detector. Each plaque was arranged with realistic multiple ^{125}I seed configurations. The measured dose distributions were compared to the corresponding dose profiles calculated with the TPS. All measurements were corrected for the angular sensitivity variation of the diode.

Results: Single-seed dose distributions measured with our dosimetry setup agreed with previously published data within 3%. For the three multiple-seed plaque configurations, the measured and calculated dose distributions were in good agreement. For the central axis depth doses, the agreement was within 4%, whereas deviations up to 11% were observed in single points far off-axis.

Conclusions: The Bebig Plaque Simulator is a reliable TPS for calculating relative dose distributions around realistic multiple ^{125}I seed configurations in EPT. © 2001 Elsevier Science Inc.

Episcleral plaque therapy, ^{125}I seeds, Dose distributions, Dose verification.

INTRODUCTION

Episcleral plaque therapy (EPT) is an attractive treatment alternative in the management of ocular malignant melanomas. A radioactive plaque is sutured to the scleral surface corresponding to the basis of the intraocular tumor (1). The plaque remains attached until a specified dose is delivered to a defined point in the tumor. At our institution, we routinely prescribe 100 Gy to the tumor apex. Several isotopes have been used in episcleral plaque therapy, e.g., ^{125}I, ^{192}Ir, and ^{106}Ru. The ^{125}I and ^{192}Ir isotopes are photon emitters, whereas ^{106}Ru emits electrons. A major advantage of using ^{125}I is that this isotope may be delivered as seeds that fit into fixed positions in some of the plaques available. Combining seed position and activity allows a customized dose distribution to be created for each individual patient. Another clinical advantage with the ^{125}I seeds is the relatively low energy of the emitted photons (2) (Table 1). Compared to external beam radiotherapy, EPT permits a localized dose delivery that allows higher doses to the tumor with greater sparing of noninvolved tissues (Fig. 1). Still, late radiation-induced side effects after EPT have been reported, such as loss of vision due to injury of the macula and optic disc, cataract, and glaucoma (3). As in other curative or radical

Reprint requests to: Rune Hafslund, Department of Radiophysics, Haukeland University Hospital, N-5021 Bergen, Norway. Tel: (+47) 5597-2057; Fax: (+47) 5597-2046; E-mail: rune.hafslund@haukeland.no.

The study was presented at the Xth International Congress of Ocular Oncology, Amsterdam, The Netherlands, 17–21 June 2001, and at the 6th Biennial ESTRO Meeting on Physics for Clinical Radiotherapy, Seville, Spain, 17–20 September 2001.

This study was supported by grants from Haukeland University Hospital and the Norwegian Cancer Society.

Acknowledgments—Mr. Dagfinn Knutsen is acknowledged for his clever and accurate production of the plaque adapters. The technical assistance with handling different image formats provided by physicist Torbjørn Frøystein, M.Sc., is also appreciated.

Received Oct 19, 2000, and in revised form Jul 11, 2001. Accepted for publication Jul 12, 2001.

Table 1. The photon energies for the model 6702 seed and the model 6711 seed*

	$^{125}I \rightarrow {}^{125}Te$ (keV)			^{109}Ag, fluorescence (keV)	
	27.4	31.4	35.5	22.1	25.2
Model 6702	76.9%	18.8%	4.3%	–	–
Model 6711	61.3%	15.3%	3.7%	15.4%	4.3%

* Data from Ref. (2).

radiotherapy practice, the risk of normal tissue toxicity limits the dose that can be safely directed at the tumor. Precise absolute and relative dosimetry is therefore fundamental for both tumor dose prescription and judgment of the risk of normal tissue toxicity.

Dedicated treatment-planning systems (TPS) are available for calculation of both absolute dose and relative dose distributions for individual tumors/seed configurations used in EPT. Measurements of the dose distribution for one or two ^{125}I seeds located in different ophthalmic plaques have been reported previously. Using thermoluminescence dosimetry, Luxton *et al.* (3) measured the dose distribution for two seeds positioned in a custom-made gold plaque, today known as a USC-type (University of Southern California) plaque; Chiu-Tsao *et al.* (4) and de la Zerda *et al.* (5) measured the dose distribution for a single seed positioned in the center of a COMS (Collaborative Ocular Melanoma Study) 20-mm plaque. Weaver (6) positioned one ^{125}I seed in different self-made plaques and compared the results with the dose distribution simulated by a computer program. Other authors have used diodes to measure the dose distribution for single ^{125}I seeds and reported that the accuracy was at least as good as the accuracy of thermoluminescence dosimetry measurements (7–11). However, in clinical practice, plaques are configured with 4–20 ^{125}I seeds. Astrahan *et al.* have compared measured and calculated *depth* doses for five ^{125}I seeds arranged in noncommercial plaques (12). In this paper, we present a verification of the depth dose and off-axis dose calculations of a commercially available dedicated TPS when realistic multiple-seed configurations are applied in standard commercially available gold plaques. The calculated dose distributions are verified against dose distributions measured with a diode detector.

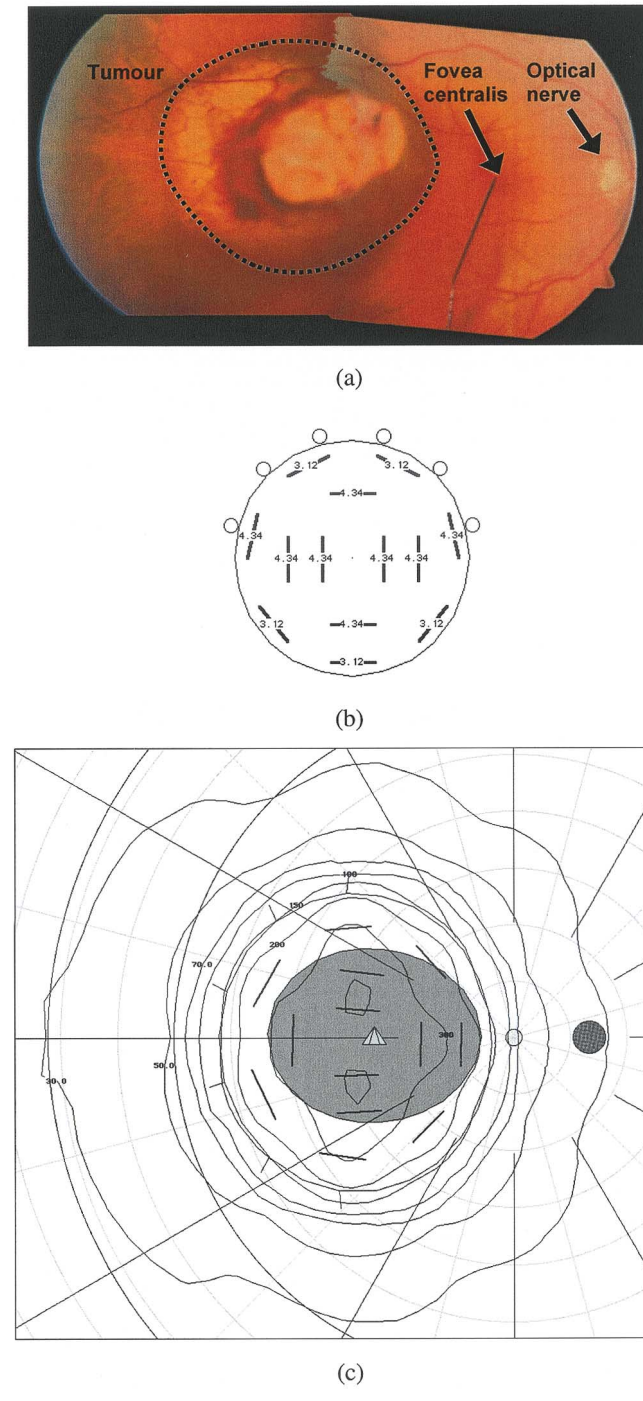

Fig. 1. Episcleral plaque brachytherapy treatment of a patient presenting with choroidal malignant melanoma in the right eye. (a) Two merged fundus images showing the choroidal melanoma (encircled) close to the macula. Centrally, the tumor has caused a bleeding and rupture of Bruch's membrane. (b) Schematic drawing of a COMS plaque with the applied seed configuration. The number shown over each seed indicates the seed activity in mCi. (c) Corresponding retinal diagram illustrating that the applied seeds produce a dose distribution that conforms closely to the defined tumor area.

MATERIALS AND METHODS

The Bebig Plaque Simulator treatment planning system

The TPS Bebig Plaque Simulator (13) is used for planning EPT at our institution. This TPS supports dose calculations for a wide range of radioactive nuclides and seed models. The user may choose arbitrary seed activity and configurations in several different commercial plaques and may also design new plaques. The dose calculations may be performed three-dimensionally and are visualized on retinal diagrams and sagittal cross-sections. Fundus images from the ophthalmoscopic examination can be merged onto the retinal diagram. By using standard export options, dose maps in arbitrary two-dimensional planes and along one-

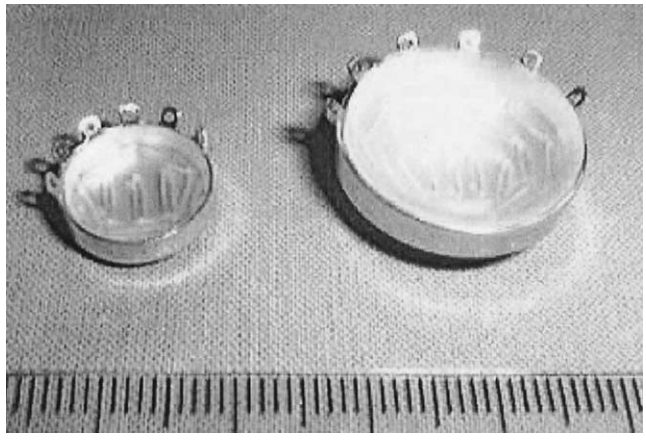

Fig. 2. The (left) COMS 12-mm and (right) COMS 20-mm plaques.

dimensional lines may be obtained in tabular format. Further details on dose calculation algorithms have been reported previously (13).

The COMS and USC eye plaques used in routine episcleral brachytherapy treatment

Common eye plaques used in routine treatment at our institution are the circular COMS plaques (14) (Fig. 2), with diameters ranging from 12 to 20 mm in steps of 2 mm, and some of the USC plaques (3) (Fig. 3). These plaques are all made to fit tumors of different sizes and locations, and some of the USC plaques are specially designed for treating tumors close to the optic nerve (1). In the COMS plaques, the seeds are embedded in grooves in a flexible silicone rubber containing fixed seed positions. This silicone seed carrier is made to fit into the gold plaque. The USC plaques do not contain silicone rubber. Instead, the seeds are glued directly into slots in the gold plaque. In this dosimetric verification study, the COMS 12-mm and 20-mm plaques and the USC#9 plaque were applied.

Fig. 3. The USC#9 plaque.

The two types of ^{125}I seeds

Two different types of commercially available ^{125}I seeds (Medi-Physics Inc., USA, now Nycomed Amersham plc, UK) were used in this study. The model 6702 seed contains ^{125}I absorbed on three resin spheres. In the model 6711 seed, ^{125}I is absorbed on the surface of a silver wire. Both the resin spheres and the silver wire are contained within a thin titanium capsule 0.8 mm in diameter and 4.5 mm long. The energies of the photons emitted from both the model 6702 seed and the model 6711 seed range from 22.1 to 35.5 keV (Table 1). The activity of the seeds applied in this study ranged from 5 to 40 mCi to improve the signal:noise ratio.

Description of the dosimetry system

A silicon p-n junction diode (Poseidon Field Detector, Precitron AB, Uppsala, Sweden) with increased sensitivity for low energies was used to measure the dose distributions in this study. The diode was made of n-type silicon and had an active/detector volume with a thickness of 0.3 mm and an area of 2.8×2.8 mm^2. The effective point of measurement of the diode was defined to be 0.5 mm below the outer diode surface. To move the diode along the lines where the dose distributions were measured and to record the signal received by the diode, we used a standard external beam water phantom dosimetry system (Wellhöfer WP700 water phantom with a WP5007 electrometer; Wellhöfer Dosimetrie, Nürnberg, Germany). A set of custom-made adapters was used to fix the three different plaques and the single seeds to the inner wall of the WP700 water phantom (Fig. 4). Errors relating to uncertainties in positioning the diode relative to a fixed point in all plaques were estimated to be less than 0.5 mm. All measurements were performed in water, and we assumed that the dose was proportional to the recorded diode signal.

Verification of the dosimetry setup through measurements on a single seed

Our dosimetry setup was verified through measurements on a single ^{125}I seed. We measured the dose distribution perpendicular to the length axis of a model 6711 seed (the central axis depth dose) and compared the results with corresponding measurements reported by Ling *et al.* (9).

Measurements and calculations of central axis depth dose and off-axis dose profiles for realistic multiple-seed configurations

Central axis depth dose and off-axis dose profiles were measured for the three plaques; for each plaque, a realistic seed configuration was applied. The central axis depth dose was defined as the dose absorbed at different depths perpendicularly from the center of the plaque. The off-axis dose profile was defined as the dose absorbed along a horizontal line at a given perpendicular distance to the central axis. These terms were applied instead of the geometry factor, radial function, and anisotropy function defined in the AAPM Task Group Report No. 43 (15) for dosimetry of single brachytherapy sources, because we considered

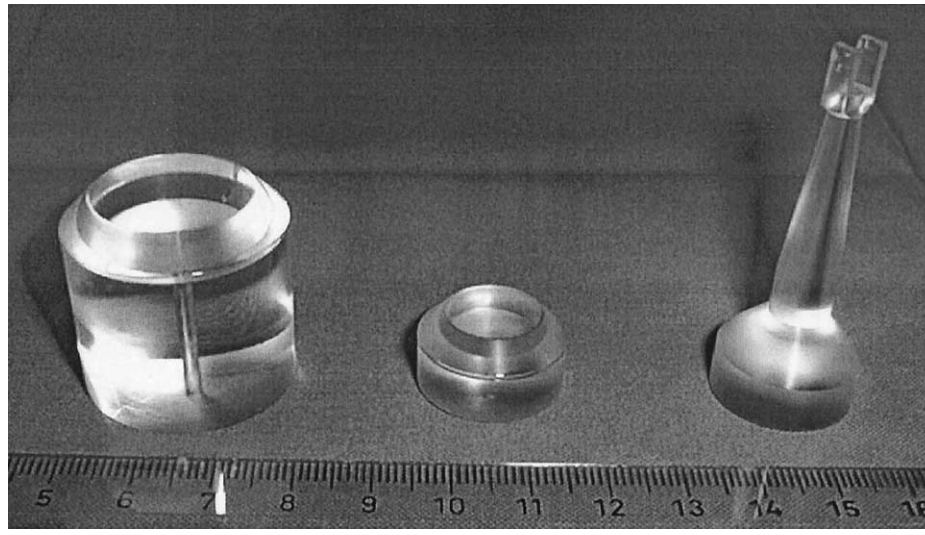

Fig. 4. The adapters used to fix the plaques to the inner wall of the water phantom. The COMS 20-mm plaque, as well as the USC#9 plaque, was fixed to the water phantom using the adapter on the left. (The USC#9 plaque was fixed through the hole in the middle.) The COMS 12-mm plaque was fixed using the adapter insert in the middle, which was put into the center of the adapter on the left. The single seed was fixed with the adapter on the right, which was also inserted into the adapter on the left.

dose distributions of multiseed configurations. To obtain correct doses, it was necessary to adjust for the angular sensitivity of the diode. All measurements were compared to calculations by the TPS, using the same plaque configurations as applied during the measurements.

Angular diode sensitivity measurements. The sensitivity of a diode detector in general depends on the angle of the incoming radiation. Thus the *angular sensitivity* of our diode was measured by moving the diode in a semicircle in the horizontal plane in front of and perpendicularly to seed axis, keeping a constant distance to the center of the seed. During these measurements, the long axis of the diode always pointed in the same direction. In our off-axis measurements, the diode moved along a straight line, and the distance between the detector and seed varied. To test if the angular sensitivity of the diode depended upon the distance between the diode and the seed, repeated sensitivity measurements were carried out, with the diode placed at three different distances (1, 1.5, and 2 cm) from the center of the seed. Measurements were performed for the angles 0°, ±30°, ±45°, ±60°, and ±90° on the semicircle.

Central axis depth dose and off-axis dose profiles of realistic plaque configurations. For all applied seed configurations in the three plaques, central axis depth dose (range

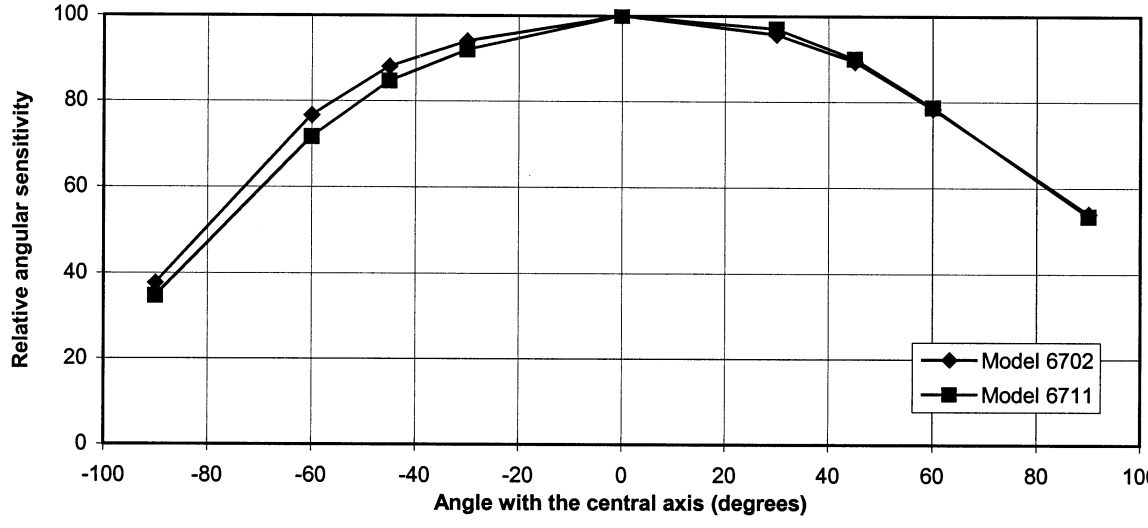

Fig. 5. The angular sensitivity of the diode used in all measurements, for both model 6702 and 6711 ^{125}I seeds. Each point in the curves is the average of three measurements with radii of 1.0 cm, 1.5 cm, and 2.0 cm from the center of the seed.

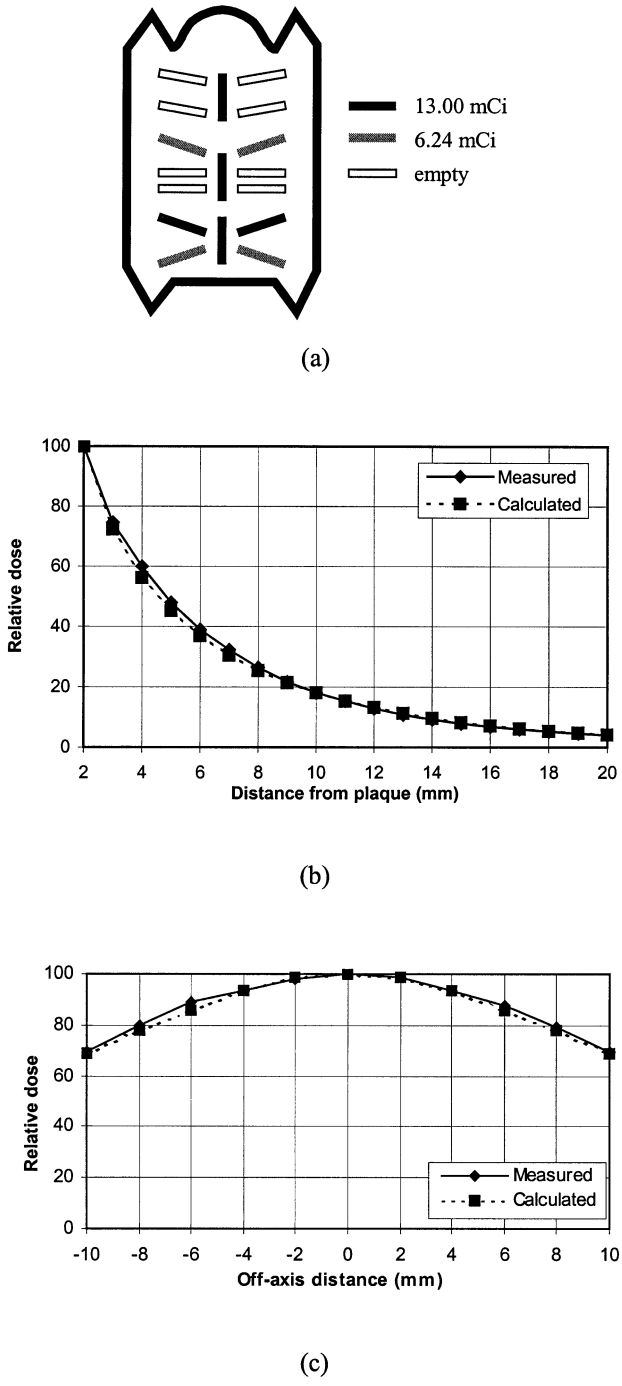

Fig. 6. (a) The model 6711 nine-seed configuration arranged in the USC#9 plaque and (b) the corresponding measured and calculated central axis depth dose and (c) off-axis dose profiles. The off-axis profiles are measured/calculated 17 mm from the center of the plaque.

2–20 mm) and off-axis dose profiles (range −10 mm to +10 mm) were recorded. Both when measuring central axis depth dose and off-axis dose profiles, the recordings were corrected for (*1*) the effective point of measurement of the diode, (*2*) the different contributions to diode signal because of different activities of the seeds, (*3*) different distance between the individual seeds and the detector using the single-seed depth dose measurements, and (*4*) the angular sensitivity of the diode. In the sensitivity corrections, adjustments were not made for the curvature of the plaques. In all seed configurations, the seeds were arranged symmetrically around the central line of the plaques.

TPS dose calculations. The dose distributions around the different plaque configurations were also calculated by the applied TPS. Both central axis depth dose and off-axis dose profiles were acquired from the calculated dose maps for comparison with the measured dose distributions.

RESULTS

The central axis depth dose of single model 6711 seed was measured to establish our dosimetry setup. Our measured data were compared to corresponding measurements done by Ling *et al.* (9). The two central axis depth doses were found to agree within approximately 3% in depth dose value at each point (data not shown).

The sensitivity of the diode decreased with increasing angle of the incoming radiation. This angular sensitivity of the applied diode was measured to obtain reliable off-axis dose profiles and was measured both for model 6702 and model 6711 seeds at three different distances from the seed (1.0 cm, 1.5 cm, and 2.0 cm). For both seed models, the diode sensitivity profile turned out to be almost independent of the distance from the seed (agreement within 5% relative to peak sensitivity). An average curve from these three different sensitivity curves was therefore used as our angular diode sensitivity profile (Fig. 5). The sensitivity was reduced to 70%–75% of the peak sensitivity at an angle of 60° (Fig. 5).

Dose measurements and calculations were carried out for three realistic multiple-seed arrangements: one configuration for each of the USC#9, COMS 12-mm, and COMS 20-mm plaques (Figs. 6–8). The number of seeds configured in the plaques ranged from 3 to 9. For all plaque and seed arrangements, the measured and calculated central axis depth dose and off-axis dose profiles were compared. Deviations up to 4% (relative to the peak dose at 2 mm) were found for central axis depth doses. For the off-axis dose profiles, the largest deviation was 11% (relative to the dose at the central axis), observed in a single point at a large angle/far from the central axis (Fig. 7c). The seed configurations and the resulting dose distributions for the plaques are shown in Figs. 6–8: The USC#9 plaque was arranged with nine model 6711 seeds (Fig. 6), the COMS 12-mm plaque consisted of eight model 6702 seeds (Fig. 7), and the COMS 20-mm plaque was configured with three model 6711 seeds (Fig. 8).

DISCUSSION

In this study we have applied a diode detector to measure the dose distribution around episcleral plaques arranged with realistic multiple ^{125}I seed configurations for the brachytherapy treatment of certain ocular tumors. The mea-

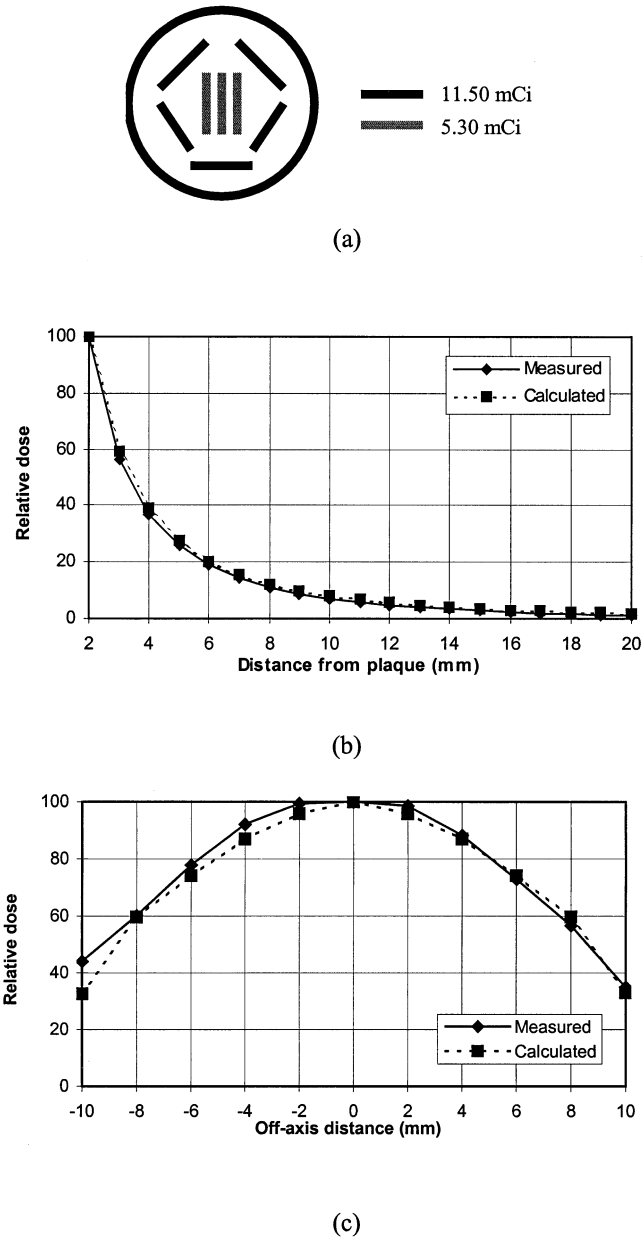

Fig. 7. (a) The model 6702 eight-seed configuration arranged in the COMS 12-mm plaque and (b) the corresponding measured and calculated central axis depth dose and (c) off-axis dose profiles. The off-axis profiles are measured/calculated 7 mm from the center of the plaque.

surements were performed to verify the performance of the TPS routinely used at our institution to plan this type of treatment.

We tested our experimental setup by measuring the central axis depth dose for a single ^{125}I seed, as previously reported by Ling *et al.* (9). Agreement within 3% was found, confirming that our dosimetry methods were adequate. This is also in concordance with previous reports on ^{125}I seed dose measurements using diode detectors (7–11).

A considerable angular sensitivity variation for the applied diode was demonstrated (Fig. 5). These fundamental characteristics of diode detectors *must* be taken into account

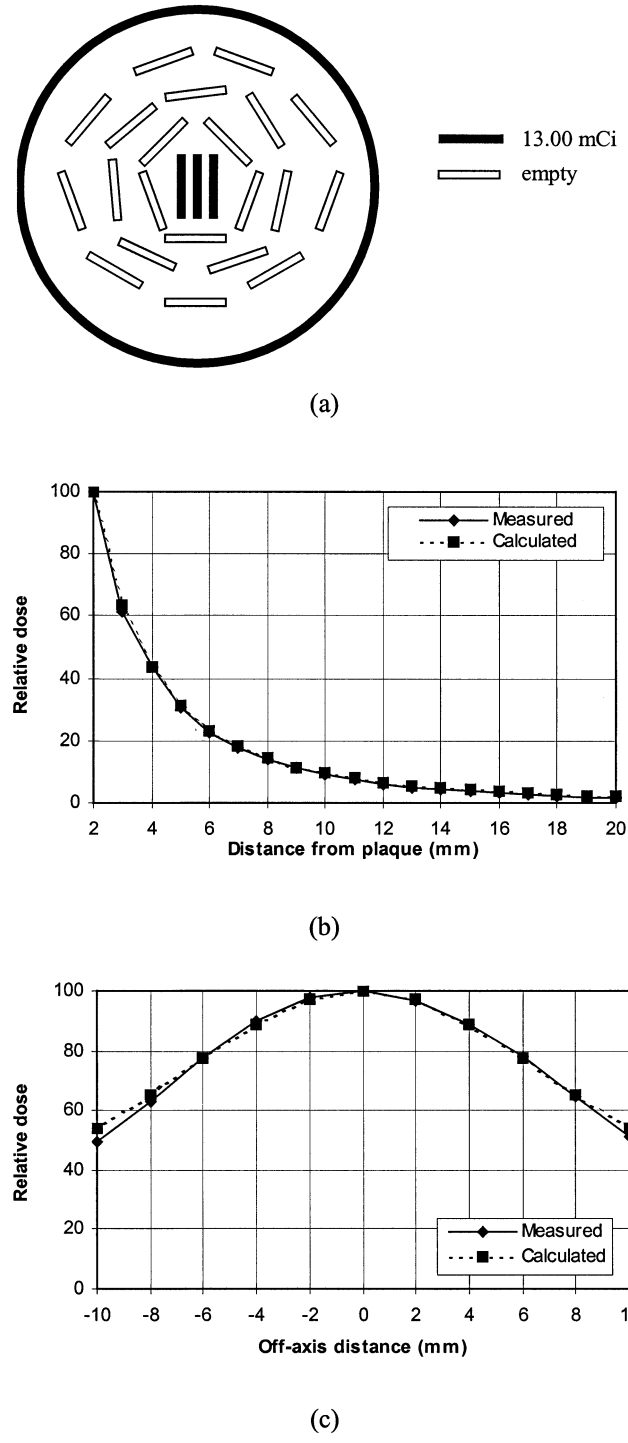

Fig. 8. (a) The model 6711 three-seed configuration arranged in the COMS 20-mm plaque and (b) the corresponding measured and calculated central axis depth dose and (c) off-axis dose profiles. The off-axis dose profiles are measured/calculated 10 mm from the center of the plaque.

to obtain reliable off-axis dose profiles. The sensitivity variation was similar for the two different seed models and was slightly asymmetrical at angles larger than 60°. This asymmetry may be explained by a small positioning error of the seed relative to the diode. Equatorial anisotropy may

have an impact on our measurements of the angular sensitivity of the diode. We checked for equatorial anisotropy (at 0°, 90°, 180°, and 270°) and found a maximum variation of 15% when measuring at different depths and integration times (data not shown). This variation was not incorporated into our angular sensitivity correction, because it was difficult to recall the exact angular positions of the seeds in the repeated daily setups. In addition, when measuring dose distributions of multiseed configurations, this interseed variation may be smoothed out. Furthermore, in our off-axis measurements, the angle with the central axis was always less than 55° (maximum off-axis measurement point was 10 mm; minimum depth was 7 mm); in most cases, the angle was less than 40°. For this reason, the large-angle asymmetry did not significantly influence our corrected off-axis dose profiles.

Because of the steep dose gradients between malignant tissue and organs at risk present in EPT, strict positioning and dosimetric accuracy requirements should be pursued. We experienced some small problems with the positioning of the seeds in the plaques, which may explain some of the deviations between the measured and calculated data. In the COMS plaque, the plaque itself may have pressed the silicon seed carrier somewhat forward (~1 mm), decreasing the distance between the diode and the seeds and contributing to spatial uncertainty in the depth dose measurements for this type of plaque. The slots in the USC#9 plaque in particular are slightly bigger than the seeds in the longitudinal direction, which may have caused small positioning errors. Because of the irregular shape of the USC#9 plaque, we also had a small problem in defining the plaque's central line relative to the wall of the water phantom.

In this study we have addressed dose distributions around *multiple* seed configurations. Precise *individual* seed activity is a prerequisite for accurate absolute dose calculations. However, the individual seed activities were also included in the corrections performed for each individual seed in the plaques to obtain true off-axis dose profiles. Uncertainties in seed activities may therefore have caused errors in the sensitivity-corrected off-axis measurements. According to the manufacturer, the uncertainty in activity for each seed within a batch was ±3.5%, whereas each batch had an uncertainty of ±5.0% in the specified activity. Because seeds from different batches were used in some of our seed configurations, these uncertainties would combine into an overall uncertainty between the individual seed activities. This uncertainty in activity is probably one of the major sources of dosimetric errors, both in this treatment planning verification study and in EPT in general. This problem could be reduced if seeds from only one batch were used in each case. However, in EPT practice, this would compromise the ability to shape the dose distribution to the targeted tumor. Improved accuracy in seed activity specification in general should therefore be a primary aim in future work.

In the dosimetric work presented in this paper, we have attempted to comply with the precise dosimetry requirements raised by the steep dose gradients present in routine episcleral plaque treatment. Our precise dosimetry implied both careful positioning of the seeds in the plaque and of the plaque itself relative to the detector. In addition, the detector signal had to be corrected for distance, seed activity, and angular diode sensitivity variation. Considering the difficult dosimetric conditions (e.g., low-energy photons, low-dose rate, and steep dose gradients), the results presented in this study demonstrate acceptable deviations between the calculated (TPS) and measured dose distributions (Figs. 6–8).

In many clinical situations, the tumor is close to sensitive structures such as the macula and optic nerve. It would therefore be of great interest to verify the dose distribution close to the plaque, where the collimating effect created by the lip and/or the slot design is used to protect these critical structures. With the limitations of our dosimetry setup (e.g., diode size, diode angular sensitivity, low seed activity, inverse-square corrections, and larger relative positioning uncertainties at short distances), we decided to restrict our measurements to depths of 7 to 17 mm if acceptable experimental accuracy should be maintained. Precise measurements close to the plaque will impose even stricter experimental conditions and is a topic for further investigations.

In conclusion, we have measured the dose distributions around realistic multiple-seed arrangements configured in episcleral therapy plaques. Dose calculations of the same seed and plaque configurations performed by the Bebig Plaque Simulator were in agreement with our experimental data. We therefore conclude that this planning system reliably calculates relative dose distributions in EPT.

REFERENCES

1. Petrovich Z, Astrahan M, Luxton G, *et al*. Primary malignant melanoma of the uvea. Radioactive plaque therapy and other treatment modalities. In: Alberti WE, Sagermann RH, editors. Radiotherapy of intraocular and orbital tumors. Berlin: Springer Verlag; 1993. p. 31–44.
2. Luxton G. Comparison of radiation dosimetry in water and in solid phantom materials for I-125 and Pd-103 brachytherapy sources: EGS4 Monte Carlo study. *Med Phys* 1994;21:631–641.
3. Luxton G, Astrahan MA, Liggett P, *et al*. Dosimetric calculations and measurements of gold plaque ophthalmic irradiators using iridium-192 and iodine-125 seeds. *Int J Radiat Oncol Biol Phys* 1988:15:167–176.
4. Chiu-Tsao ST, Anderson LL, O'Brian K, *et al*. Dosimetry for ^{125}I seeds (model 6711) in eye plaques. *Med Phys* 1993;20: 383–389.
5. de la Zerda A, Chiu-Tsao ST, Lin J, *et al*. ^{125}I eye plaque dose distribution including penumbra characteristics. *Med Phys* 1996;23:407–417.
6. Weaver KA. The dosimetry of ^{125}I seed eye plaques. *Med Phys* 1986;13:78–83.
7. Chiu-Tsao ST, Anderson LL, O'Brian K, *et al*. Dose rate determination for ^{125}I seeds. *Med Phys* 1990;17:815–825.
8. Cygler J, Szanto J, Soubra M, *et al*. Effects of gold and silver backings on the dose rate around an ^{125}I seed. *Med Phys* 1990;17:172–178.

9. Ling CC, Schell MC, Yorke E, *et al*. Two-dimensional dose distribution of ^{125}I seeds. *Med Phys* 1985;12:652–655.
10. Meli JA, Motakabbir KA. The effect of lead, gold and silver backings on dose near ^{125}I seeds. *Med Phys* 1993;20:1251–1256.
11. Schell MC, Ling CC, Gromadzki ZC, *et al*. Dose distribution of model 6702 I-125 seeds in water. *Int J Radiat Oncol Biol Phys* 1987;13:795–799.
12. Astrahan MA, Luxton G, Qiang P, *et al*. Conformal episcleral plaque therapy. *Int J Radiat Oncol Biol Phys* 1997;39:505–519.
13. Astrahan MA, Luxton G, Jozsef G, *et al*. An interactive treatment planning system for ophthalmic plaque radiotherapy. *Int J Radiat Oncol Biol Phys* 1990;18:679–687.
14. Kline RW, Yeakel PD. Ocular melanoma, I-125 plaques (Abstr.). *Med Phys* 1987;14:475.
15. Nath R, Anderson LL, Luxton G, *et al*. Dosimetry of interstitial brachytherapy sources: Recommendations of the AAPM Radiation Therapy Committee Task Group No. 43. American Association of Physicists in Medicine. *Med Phys* 1995;22:209–234.